Monostable array-enhanced stochastic resonance

John F. Lindner,[1,2] Barbara J. Breen,[2] Meghan E. Wills,[1] Adi R. Bulsara,[3] and William L. Ditto[4]
[1]*Department of Physics, The College of Wooster, Wooster, Ohio 44691-2363*
[2]*School of Physics, Georgia Institute of Technology, Atlanta, Georgia 30332-0430*
[3]*Space and Naval Warfare Systems Center, Code D364, San Diego, California 92152-5001*
[4]*Georgia Tech/Emory Department of Biomedical Engineering, Atlanta, Georgia 30332-0535*
(Received 31 July 2000; revised manuscript received 17 January 2001; published 18 April 2001)

We present a simple nonlinear system that exhibits *multiple* distinct stochastic resonances. By adjusting the noise and coupling of an array of underdamped, monostable oscillators, we modify the array's natural frequencies so that the spectral response of a typical oscillator in an array of N oscillators exhibits $N-1$ different stochastic resonances. Such families of resonances may elucidate and facilitate a variety of noise-mediated cooperative phenomena, such as noise-enhanced propagation, in a broad class of similar nonlinear systems.

DOI: 10.1103/PhysRevE.63.051107 PACS number(s): 05.40.Ca, 02.50.−r, 87.80.−y

I. INTRODUCTION

Stochastic resonance (SR) is a dynamic, noise-mediated, nonlinear phenomenon. The canonical example [1] involves an overdamped but sinusoidally driven, noisy, bistable oscillator. Adjusting the noise intensity, so that the average rate of hopping between the stable states is (approximately) twice the drive frequency, maximizes the response of the system, as measured by the spectral power at the drive frequency $S[f_D]$ or by a suitable signal-to-noise ratio (SNR). Indeed, a hallmark of canonical SR is a local maximum in SNR as a function of noise.

Since its discovery almost two decades ago, SR has been extended in many directions [2]. For example, the overdamped, bistable potential has been replaced by an *under*-damped, monostable (quartic) potential [3]. Such a system has a natural (or characteristic) frequency dependent on the initial amplitude, and hence on the energy, of the oscillator. Adjusting the noise intensity, so that the average energy causes the natural frequency to coincide with the drive frequency, maximizes the spectral response of the system, as measured (for example) by $S[f_D]$. Recent work [4] has realized both this resonant behavior *and* canonical SR in a single underdamped bistable oscillator. SR has also been observed in special, time-varying, monostable potentials [5].

Alternatively, individual overdamped, *bistable* stochastic resonators have been coupled together in arrays [6,7]. The spectral response of a stochastic resonator coupled into an array of similar elements can significantly exceed that of an isolated stochastic resonator. If the noise and coupling are both adjusted to establish the appropriate spatiotemporal organization, then the spectral response of the coupled oscillator to a sinusoidal signal is greatly enhanced. A signature of array-enhanced SR (AESR) is a local maximum in SNR as a function of both noise and coupling, manifested (for example) in a single peak or ''resonant island'' in a contour plot of SNR as a function of noise and coupling [7]. Such arrays can also exhibit noise-enhanced propagation (NEP) [8], where moderate noise significantly extends the propagation of a signal through the array.

In this work, we study noise-mediated resonant behavior in a simple array of underdamped, symmetric but nonlinear, monostable oscillators. We demonstrate how to tune noise intensity and coupling strength to adjust the natural frequencies of the individual elements in the array so as to amplify the spectral power at particular frequencies. We show that the spectral response of a typical oscillator coupled into an array of N oscillators may exhibit $N-1$ such *intrawell* stochastic resonances (adopting the language of [4]), each resonance distinguished by a unique coupling. (Stochastic multiresonance has been observed before, but in more complicated, time-varying potentials [9].) These families of resonances may have practical implications for the design of signal-processing arrays and might be observable in the resonant vibrations of impure crystals, or in anomalously long propagation of signals in noisy media.

II. NUMERICAL TECHNIQUES

Consider an array of noisy driven oscillators whose nth element is specified by the equilibrium coordinate $x_n[t]$, which evolves according to

$$m\ddot{x}_n+\gamma\dot{x}_n=-V'[x_n]+A_D\sin[2\pi f_D t]+\sigma N_n[t] +\kappa\nabla^2 x_n, \quad n=1,\ldots,N. \tag{1}$$

The accent denotes differentiation with respect to position and the overdots indicate differentiation with respect to time. The nonlinear potential $V[x]=\frac{1}{2}\alpha x^2+\frac{1}{4}\beta x^4$ is monostable for $\alpha,\beta>0$. The stochastic term $N_n[t]$ represents (band-limited) white noise with zero mean and unit root-mean-square amplitude. The noise is uncorrelated from site to site. The discrete Laplacian $\nabla^2 x_n=x_{n-1}-2x_n+x_{n+1}$ implements local linear coupling. The phantom oscillators $x_0\equiv x_1$ and $x_{N+1}\equiv x_N$ enforce free boundary conditions.

Throughout this work, we fix the inertia and viscosity parameters, $m=1$ and $2\Gamma\equiv\gamma=0.01$. We also fix the shape of the potential, $\alpha=1$ and $\beta=0.1$. However, we vary—and tune—the noise and coupling amplitudes σ and κ. We consider weak drives, $A_D\ll\sigma$ with $f_D\sim 1$, so that the spectral responses are relatively simple, with only N prominent natural frequencies.

We numerically integrate [10] the stochastic differential Eq. (1) with a small time step $dt=T_D/2^{10}$, the Gaussian

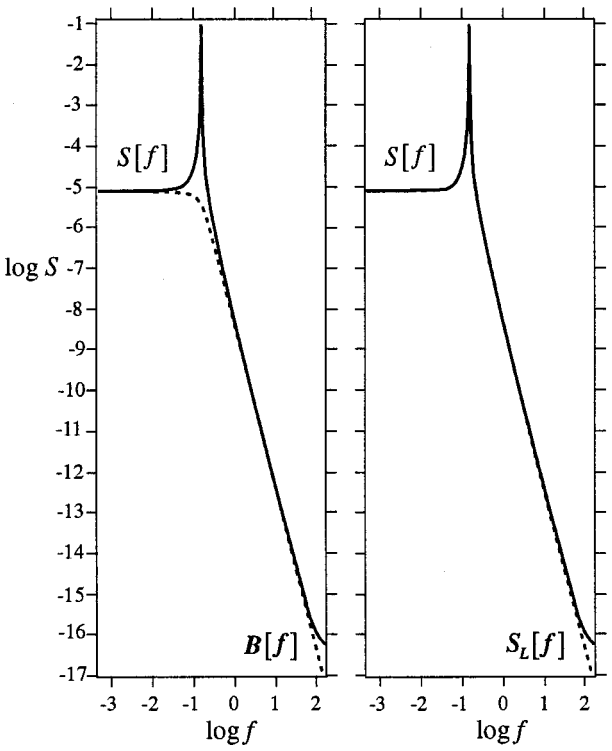

FIG. 1. On the left, a typical low-noise spectrum $S[f]$ (solid curve) of a nonlinear monostable oscillator consists of a single prominent natural frequency peak on a smooth background $B[f]$ (dotted curve). On the right, a numerically computed low-noise spectrum $S[f]$ (solid) agrees well with the corresponding linearized theoretical spectrum $S_L[f]$ (dotted). All logarithms are base ten. Parameters are $m=1$, $\gamma=0.01$, $\alpha=1$, $\beta=0.1$, $A_D=0$, $f_D=0.285$, and $\sigma^2=0.001$.

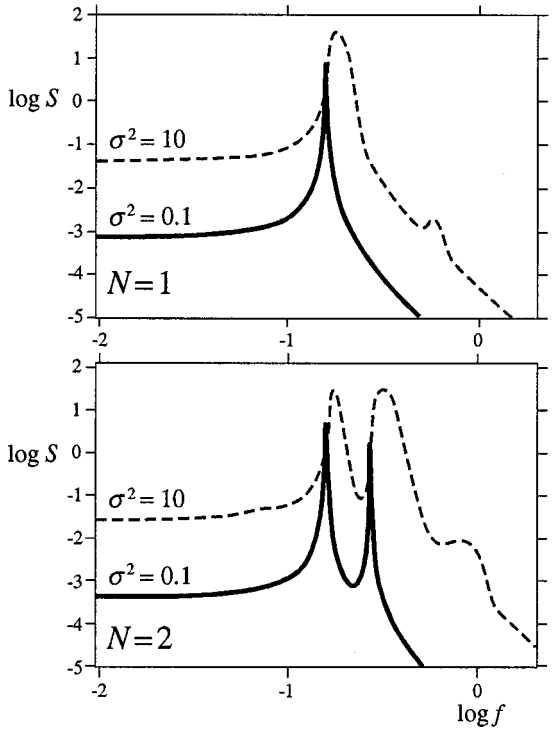

FIG. 2. Closeups of typical spectra for $N=1$ (isolated) and $N=2$ (coupled) nonlinear monostable oscillators, for low (solid) and high (dashed) noise. The $N=2$ spectrum includes two prominent natural frequency peaks, corresponding to the symmetric and antisymmetric modes of the corresponding linearized oscillators. (At high noise, additional minor peaks centered at nonlinear overtones appear.) Other parameters are as in Fig. 1, but with coupling $\kappa=1$ for the $N=2$ spectrum, and noise variance as indicated.

noise being generated via the Box-Muller algorithm [11] and a pseudorandom number generator. We estimate the mean-square amplitude per frequency (or power spectrum) $S[f]$ by averaging the spectra of many segments of a long time series of the nth oscillator of the array. Each spectrum is normalized so that the bounded area is the total mean-square amplitude. We find the spectra of all oscillators in an array to be qualitatively similar, except for the middle oscillator (when it exists), which exhibits fewer spectral peaks.

III. WEAK-NOISE THEORY

For weak drives, a typical spectrum $S[f]$ of an isolated $N=1$ oscillator consists of a single prominent natural frequency peak superimposed on a smooth background. In fact, if the noise is sufficiently weak so that the oscillator is not driven beyond its linear regime, then for vanishing driving, we can solve the linearized Eq. (1) for the Fourier transform of the time series $\tilde{x}[f]$ and write

$$S_L[f] \propto |\tilde{x}[f]|^2 \propto \frac{1}{m^2(f^2-f_0^2)^2+\gamma^2 f^2}, \tag{2}$$

where $f_0=\sqrt{\alpha/m}$ is the natural frequency of the system. Figure 1 compares the theoretical linearized spectrum of Eq. (2), suitably normalized, with a numerically computed spectrum for low noise. The agreement is excellent, except for a slight rise in the high-frequency tail of the computational spectrum, which is an unavoidable aliasing artifact [11]. It is worth noting that alternative stochastic linearization techniques [12] can be readily applied to the $N=1$ case, yielding corrections to Eq. (2) for small deviations from linearity.

For weak drives, a typical spectrum $S[f]$ of a coupled $N=2$ oscillator consists of *two* prominent natural frequency peaks superimposed on a smooth background. These peaks correspond to symmetric (in-phase) and antisymmetric (antiphase) modes of the array. For sufficiently weak noise and vanishing driving amplitude, we can again explicitly represent the spectrum, this time as

$$S_L[f] \propto \frac{1}{m^2(f^2-f_0^2)^2+\gamma^2 f^2} + \frac{1}{m^2(f^2-f_1^2)^2+\gamma^2 f^2}, \tag{3}$$

where $f_0=\sqrt{\alpha/m}$ is the frequency of the coupling-independent symmetric mode and $f_1=\sqrt{(\alpha+3\kappa)/m}$ is the higher frequency of the coupling-dependent antisymmetric mode. Theory and computation are again in excellent agreement. Figure 2 provides example spectra at low and high noise for both $N=1$ and $N=2$. Note the rise (in the back-

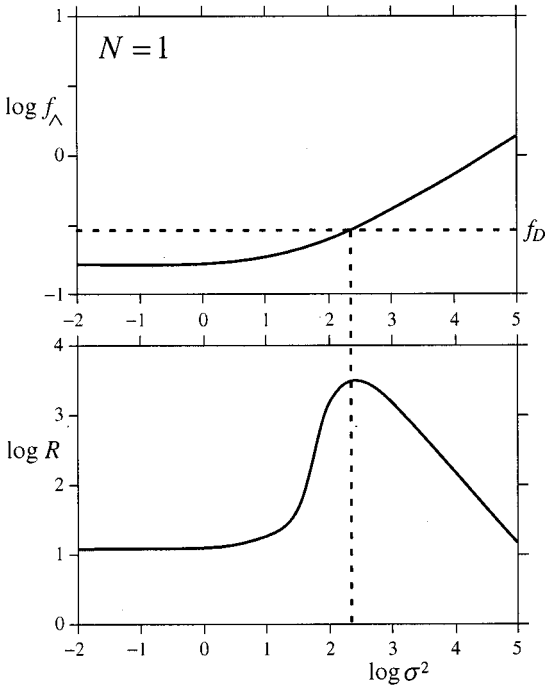

FIG. 3. Shift in natural frequency peak f of an $N=1$ oscillator with noise. As the peak shifts to larger frequencies, it induces a local maximum in the spectral response $R=S[f_D]/B[f_D]$ at the drive frequency f_D, which is indicated by the dashed line.

ground) and the shift and broadening of the peaks with increasing noise. (At higher noise, additional peaks centered at overtones of the natural frequency appear.)

Although analytic techniques can generate (typically elaborate) expressions for the shapes of the spectral peaks [13], a simple theory can readily capture their movements, and this is sufficient for our purposes. If we momentarily neglect damping and driving, we may estimate the natural frequency of the nonlinear monostable oscillator by integrating the energy expression $E=\frac{1}{2}m\dot{x}^2+V[x]$ between the classical turning points $x_{\pm}[E]$ to get the nonlinear dispersion relation

$$\frac{1}{f[E]}=T[E]=2\sqrt{m/2}\int_{x_-[E]}^{x_+[E]}\frac{dx}{\sqrt{E-V[x]}}, \tag{4}$$

where the turning points may be calculated via the implicit relationship $V[x_{\pm}]=E$. Although the integral in Eq. (4) can be performed analytically, it is more convenient to numerically integrate it for a range of energies. Returning to the full equation of motion, including damping and driving, at steady state, we find dimensionally and numerically that the average energy is proportional to the mean-square amplitude of the noise $\langle E\rangle\sim 2\sigma^2\tau/\gamma=D/\Gamma$. This enables us to predict the position of the natural frequency peak f_Λ as a function of noise. Theory and computation are in excellent agreement.

IV. MODERATE NOISE

For small noise $\sigma^2\ll\alpha^3/\beta$, the natural peak of an isolated $N=1$ oscillator is fixed, but for large noise $\sigma^2\gg\alpha^3/\beta$, the peak shifts to higher frequencies and broadens. Provided the nonlinearity is nonzero ($\beta>0$), increasing noise will cause the natural frequency peak to shift to increasingly large frequencies, as illustrated by the top graph in Fig. 3. This shift generates an enhanced response to a weak drive when the natural frequency peak centers on the drive frequency. We measure this response by the ratio of the spectrum $S[f]$ at

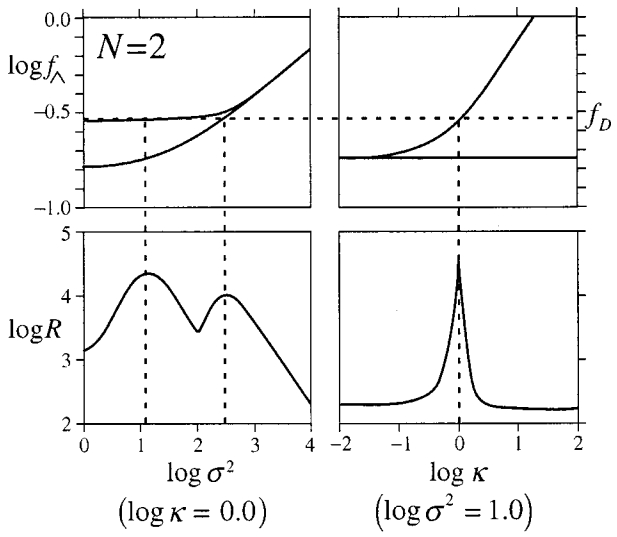

FIG. 4. Shift in the natural frequencies of an $N=2$ oscillator with noise and coupling. At a given drive frequency f_D, indicated by the horizontal dashed line, the noise-induced shift (top left) induces two local maxima in the SNR, as a function of noise (bottom left), while the coupling-induced shift (top right) induces one local maximum as a function of coupling (bottom right).

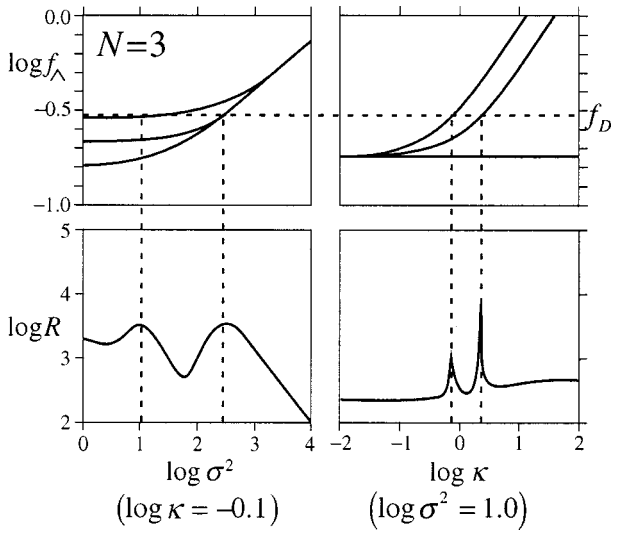

FIG. 5. Shift in the natural frequencies of an $N=3$ oscillator with noise and coupling. At a given drive frequency f_D, indicated by the horizontal dashed line, the noise-induced shift (top left) induces two local maxima in the SNR, as a function of noise (bottom left), while the coupling-induced shift (top right) induces two local maxima as a function of coupling (bottom right).

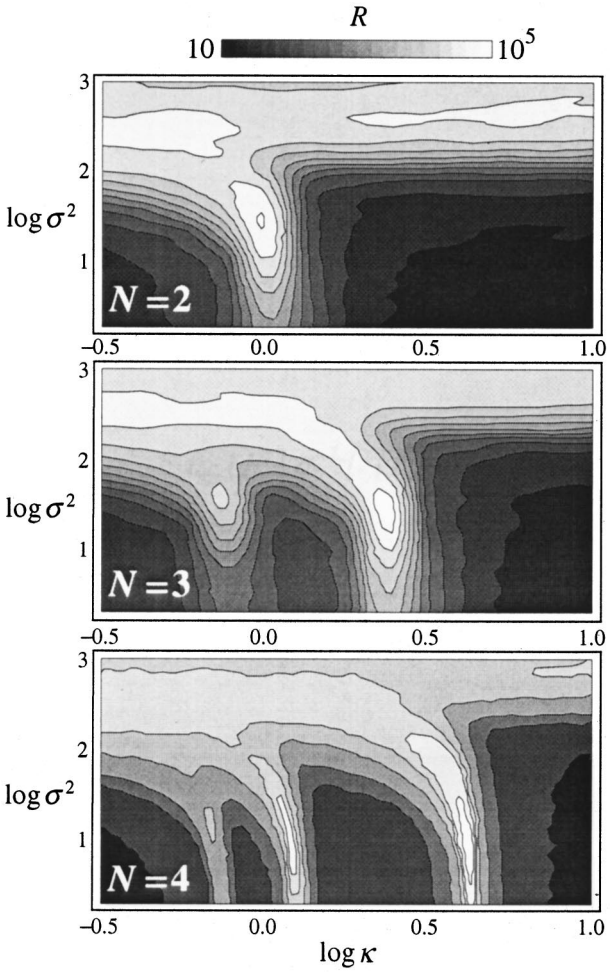

FIG. 6. Contour plots of the spectral responses R, as a function of ''local'' noise σ^2 and coupling κ, for oscillators at the ends of $N=2$, 3, and 4 arrays. The drive frequencies are $f_D=0.285$, 0.3, and 0.3, respectively. In each case, there are $N-1$ local maxima.

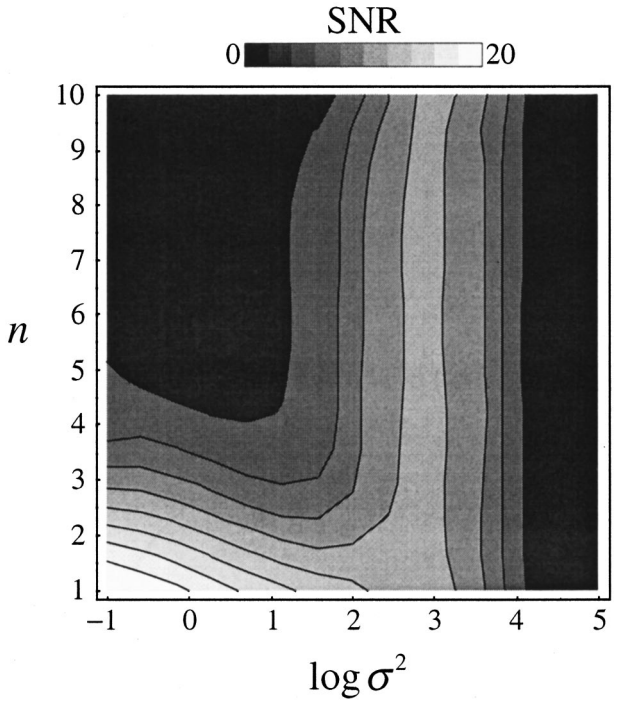

FIG. 7. When driven sinusoidally only at one end ($n=1$), arrays of monostable nonlinear oscillators also exhibit NEP. Smoothed contour plot of SNR as a function of noise variance σ^2 and oscillator number n. Intermediate noise optimizes the propagation of the signal. Parameters are $m=1$, $\gamma=5\times10^{-5}$, $\alpha=1$, $\beta=1$, $A_D=1$, $f_D=0.45$, and $\kappa=1$.

the drive frequency to the smooth background $B[f]$ at the drive frequency, $R\equiv S[f_D]/B[f_D]$. This measure is faithful to the squared ''stochastic amplification factor'' originally employed to describe monostable SR [3], and it best exhibits the generalization of the phenomenon to arrays. We can calculate R with vanishing drive amplitude because R measures whether or not, and to what extent, a *natural frequency peak* is at the drive frequency, and because this frequency matching is the essential ingredient of monostable SR. The response R is illustrated in the bottom graph of Fig. 3, where it is maximized when the natural frequency peak shifts to the drive frequency, as indicated by the dashed lines.

A similar but richer situation exists for *arrays* of nonlinear monostable oscillators. Consider next the case $N=2$. A typical spectrum, derived from the time series of either oscillator, now consists of two natural frequency peaks, corresponding to the symmetric and antisymmetric modes, riding on top of a smooth background. We can again predict the shift of the peaks, this time with respect to *both* noise *and* coupling, as indicated in Fig. 4. For sufficiently large frequencies, there exists one local maximum in R as a function of coupling, due to the drift of the antisymmetric mode peak. Also, for sufficiently large frequencies, there are *two* local maxima in R as a function of noise. This result is a single local maximum in the noise-coupling plane. The top contour plot of Fig. 6 summarizes the spectral response, where a low noise ''island'' accompanies a high-noise ''ridge.''

For $N=3$, a typical spectrum, derived from the time series of either end oscillator, consists of *three* natural frequency peaks riding on top of a smooth background. Due to the shift of the peaks with noise and coupling, for sufficiently large frequencies, we expect *two* local maxima in R as a function of coupling (due to the drift of the nonsymmetric modes) and *three* local maxima in R as a function of noise. However, peak broadening due to nonlinear dispersion at high noise consolidates the peaks, limiting the number of local maxima in R as a function of noise to two, as indicated in Fig. 5. This induces two local maxima in the noise-coupling plane (for f_D just above the zero-noise natural frequencies). The middle contour plot of Fig. 6 summarizes the spectral response, where two low-noise islands accompany a high-noise ridge. The bottom contour plot of Fig. 6 is for $N=4$, where there are three low-noise islands.

In this way, the spectra of typical oscillators in an array of N oscillators exhibit $N-1$ distinct resonant local maxima as a function of noise and coupling. Similar results are obtained for moderate drive amplitudes $A_D\lesssim\sigma$. However, for large drive amplitudes $A_D\gg\sigma$, the spectral responses are much more complicated. Large-amplitude drives induce many non-

linear peaks in the spectra, thereby complicating efforts to succinctly summarize the dynamics.

V. NOISE-ENHANCED PROPAGATION

Recent studies have demonstrated that noise can sustain propagation in a variety of numerical and experimental nonlinear systems [8], including arrays of bistable oscillators. Here, we note that NEP is also obtained in arrays of monostable oscillators. The numerical model is like that of Eq. (1), except only the initial oscillator is sinusoidally forced. By recording a signal-to-noise ratio at each oscillator in the array, we demonstrate that moderate noise significantly extends the propagation of the sinusoidal input. For oscillators near the forcing end, the SNR decreases as the noise increases. But for oscillators farther away, the SNR goes through a local maximum as the noise increases, which is the signature of a classic stochastic resonance. Oscillators near the forcing end do not need help from the noise, as the forcing amplitude there is large; however, oscillators far from the forcing do need help from the noise, as the signal there is attenuated. For a given noise power, SNR decreases with oscillator number, downstream along the chain. Defining the *propagation length* as the number of oscillators (or distance along the chain) for which the SNR exceeds a certain fixed cutoff, we observe that the propagation length is longest for moderate noise.

These data can be succinctly combined into a contour plot of SNR versus noise variance versus oscillator number, as in Fig. 7. Gray levels code SNR, with white indicating large SNR and black indicating small SNR. The bottom-left corner represents the peak SNR of the first oscillator. The SNR decreases everywhere away from this corner. However, the distinct bulges in the contours, where regions of large SNR extend toward the free end of the chain, are the signatures of NEP. When the noise variance $\sigma^2 \sim 10^3$, the SNR extension reaches the end of the chain, indicating that intermediate noise has succeeded in sustaining the signal throughout its length.

VI. CONCLUSIONS

Arrays of monostable oscillators exhibit multiple stochastic resonances, each resonance distinguished by a different coupling. In the absence of nonlinearity ($\beta = 0$), the natural frequency peaks do not shift to higher frequencies with noise, and the resonant islands in the noise-coupling plane disappear. The abundance of these resonances suggests phenomenology richer than that of arrays of overdamped bistable oscillators, which exhibit only a single local maximum (in SNR) as a function of noise and coupling [7]. Furthermore, having also observed NEP in monostable arrays, we anticipate that such arrays can exhibit interesting signal processing as well as novel signal propagation. Certainly, monostable arrays provide excellent examples of how noise and coupling can cooperate to induce multiple nonlinear resonances.

ACKNOWLEDGMENTS

J.F.L. thanks The College of Wooster for making possible his sabbatical at Georgia Tech. W.L.D. and A.R.B. acknowledge the Office of Naval Research, Physical Sciences Division for support. We thank Matt Wolf and the Interactive High Performance Computing Laboratory of the College of Computing at Georgia Tech. This work was supported in part by NSF Grant No. DMR-9619406.

[1] R. Benzi, A. Sutera, and A. Vulpiani, J. Phys. A **14**, L453 (1981); C. Nicolis and G. Nicolis, Tellus **33**, 225 (1981).

[2] For reviews of SR, consult K. Wiesenfeld and F. Moss, Nature (London) **373**, 33 (1995); A. R. Bulsara and L. Gammaitoni, Phys. Today **49** (3), 39 (1996); L. Gammaitoni, P. Hänggi, P. Jung, and F. Marchesoni, Rev. Mod. Phys. **70**, 223 (1998).

[3] N. G. Stocks, N. D. Stein, and P. V. E. McClintock, J. Phys. A **26**, L385 (1993); N. G. Stocks, N. D. Stein, S. M. Soskin, and P. V. E. McClintock, *ibid.* **25**, L1119 (1992).

[4] L. Alfonsie, L. Gammaitoni, S. Santucci, and A. Bulsara, Phys. Rev. E **62**, 299 (2000).

[5] J. M. G. Vilar and J. M. Rubí, Phys. Rev. Lett. **77**, 2863 (1996).

[6] P. Jung, U. Behn, E. Pantazelou, and F. Moss, Phys. Rev. A **46**, R1709 (1992); A. R. Bulsara and G. Schmera, Phys. Rev. E **47**, 3734 (1993); M. E. Inchiosa and A. R. Bulsara, *ibid.* **52**, 327 (1995); A. Neiman and L. Schimansky-Geier, Phys. Lett. A **197**, 397 (1995).

[7] J. Lindner, B. Meadows, W. Ditto, M. Inchiosa, and A. Bulsara, Phys. Rev. Lett. **75**, 3 (1995); Phys. Rev. E **53**, 2081 (1996); M. Löcher, G. A. Johnson, and E. R. Hunt, Phys. Rev. Lett. **77**, 4698 (1996); M. Löcher, D. Cigna, E. Hunt, G. Johnson, F. Marchesoni, L. Gammaitoni, and A. Bulsara, Chaos **8**, 604 (1998); A. Sarmiento, R. Reigada, A. H. Romero, and K. Lindenberg, Phys. Rev. E **60**, 5317 (1999).

[8] P. Jung and G. Mayer-Kress, Phys. Rev. Lett. **74**, 2130 (1995); S. Kádár, J. Wang, and K. Showalter, Nature (London) **391**, 770 (1998); M. Löcher, D. Cigna, and E. R. Hunt, Phys. Rev. Lett. **80**, 5212 (1998); Y. Zhang, G. Hu, and L. Gammaitoni, Phys. Rev. E **58**, 2952 (1998); J. F. Lindner, S. Chandramouli, A. R. Bulsara, M. Löcher, and W. L. Ditto, Phys. Rev. Lett. **81**, 5048 (1998).

[9] J. M. G. Vilar and J. M. Rubí, Phys. Rev. Lett. **78**, 2882 (1997).

[10] R. F. Fox, I. R. Gatland, R. Roy, and G. Vemuri, Phys. Rev. A **38**, 5938 (1988).

[11] W. H. Press, S. A. Teukolsky, W. T. Vetterling, and B. P. Flannery, *Numerical Recipes in C* (Cambridge University Press, New York, 1992).

[12] See, e.g., A. Bulsara, K. Lindenberg, and K. Shuler, J. Stat. Phys. **27**, 787 (1982); A. Bulsara, K. Lindenberg, K. Shuler, R. Frehlich, and W. Coles, Int. J. Non-Linear Mech. **17**, 237 (1982); J. Roberts and P. Spanos, *ibid.* **21**, 111 (1986).

[13] M. I. Dykman and M. A. Krivoglaz, Phys. Status Solidi B **48**,

497 (1971); Physica A **104**, 495 (1980); M. I. Dykman, R. Mannella, P. V. E. McClintock, S. M. Soskin, and N. G. Stocks, Phys. Rev. A **42**, 7041 (1990).

[14] P. Jung and G. Mayer-Kress, Phys. Rev. Lett. **74**, 2130 (1995); M. Löcher, D. Cigna, and E. R. Hunt, *ibid.* **80**, 5212 (1998); Y. Zhang, G. Hu, and L. Gammaitoni, Phys. Rev. E **58**, 2952 (1998); J. F. Lindner, S. Chandramouli, A. R. Bulsara, M. Löcher, and W. L. Ditto, Phys. Rev. Lett. **81**, 5048 (1998).